Chinese Chemical Letters 33 (2022) 4053–4056

Contents lists available at ScienceDirect

Chinese Chemical Letters

journal homepage: www.elsevier.com/locate/cclet

Development and evaluation of a thermostatic nucleic acid testing device based on magnesium pyrophosphate precipitation for detecting *Enterocytozoon hepatopenaei*

Zhu Chen[a,d,*], Kaixuan Zhao[a], Ziyu He[b], Xiaofang Luo[f], Zuodong Qin[f], Yimin Tan[a,d], Xiangming Zheng[c,d], Zuozhong Wu[e], Yan Deng[a], Hui Chen[a], Yuan Guo[b,*], Song Li[a,d,*]

[a] *Hunan Key Laboratory of Biomedical Nanomaterials and Devices, Hunan University of Technology, Zhuzhou 412007, China*
[b] *Department of Cardiovascular Medicine, The Affiliated Zhuzhou Hospital Xiangya Medical College, Central South University, Zhuzhou 412000, China*
[c] *Institute of Supramolecular Structures and Micro-nano Materials, Hunan University of Technology, Zhuzhou 412007, China*
[d] *National & Local Joint Engineering Research Center for Research and Technology of Advanced Packaging Materials, Hunan University of Technology, Zhuzhou 412007, China*
[e] *Hunan Shengzhou Biotechnology Ltd., Zhuzhou 412000, China*
[f] *College of Chemistry and Bioengineering, Hunan University of Science and Engineering, Yongzhou 425199, China*

ARTICLE INFO

Article history:
Received 7 October 2021
Revised 17 January 2022
Accepted 25 January 2022
Available online 1 February 2022

Keywords:
Turbidity detection
Magnesium pyrophosphate precipitation
Nucleic acid testing
Enterocytozoon hepatopenaei
Loop-mediated isothermal amplification

ABSTRACT

Enterocytozoon hepatopenaei (EHP) infection has seriously affected prawn culture globally. The symptoms of the infection are not apparent, and traditional detection methods are time consuming and low in accuracy. We developed a new onsite rapid testing device (size $18.8 \times 16.7 \times 6.6$ cm^3) for EHP based on magnesium pyrophosphate precipitation and facilitated by loop mediated isothermal amplification (LAMP). The design and fabrication of the device enables efficient light absorbance. The device has a highly sensitive detector, high-precision thermal controller, and humanized touch screen. The temperature control precision of the device is 0.2–0.3 °C at 60 °C, 63 °C, and 65 °C. The coefficients of variation values (CVV) of the luminous power in one channel at light on and off were found to be 0.0097 and 0.0014, respectively, within 1 h. The CVV of the background, luminous power, and values of eight PCR tubes filled with pure water were all less than 5%. In the EHP experiment, eight samples (including seven positive and one negative) confirmed the effectiveness of the device, and four positive and four negative samples verified whether cross-contamination exists. Among them, the rise time of the curve was about 15 min. These results assert that the developed device exhibits enhanced stability and uniformity and has excellent performance with high sensitivity, good specificity, and low testing time. Moreover, the optimal and minimum absorbance range was 555–655 nm for monitoring the production of LAMP.

Enterocytozoon hepatopenaei (EHP) is an obligate intracellular parasite that can infect a variety of eukaryotes, including cultured shrimps such as *Penaeus monodon* and *Litopenaeus vannamei* (LV) [1]. It has been reported that EHP infects the hepatopancreas of Penaeus but does not cause acute and large-scale death like the acute hepatopancreas necrosis caused by white spot syndrome and yellow-head disease [2]. Penaeus infected by EHP show normal feeding; however, the body color, stomach and intestines are obviously abnormal. The body color becomes white, intestinal absorption is lowered, hepatopancreatic atrophy is seen, and some LV excrete white feces. Therefore, this disease is difficult to identify in the early stage, and low or no growth becomes apparent only after 30–45 days, resulting in feed loss and seriously impacting the production. EHP can spread vertically through fertilized eggs and shrimp larvae or horizontally through contaminated aquaculture waters [3,4]. At present, it is difficult to completely achieve EHP clearance in prawns, and no effective prevention or treatment has been documented [5,6]. Eliminating the route of infection can successfully prevent infection. By quarantining the affected parent and young shrimps, the pathogens can be identified early, thereby preventing the infection of healthy shrimps and protecting the fundamental interests of the prawn breeding industry. Owing to the small size of the EHP spores, the symptoms are not obvious in the infected prawns; hence, it is difficult to confirm the diagnosis in the field [7]. Furthermore, traditional morphological methods have

* Corresponding authors.
E-mail addresses: chenzhu@hut.edu.cn (Z. Chen), guoyuan8141@csu.edu.cn (Y. Guo), solisong@163.com (S. Li).

https://doi.org/10.1016/j.cclet.2022.01.072
1001-8417/

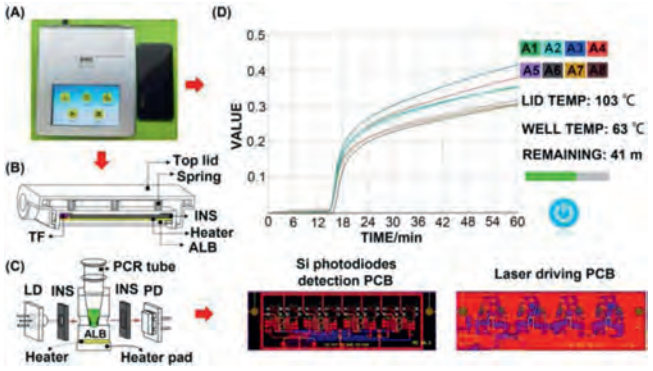

Fig. 1. (A) The design of the diagnostic device. (B) Heating cover module. (C) Reaction module. (D) Touch screen interfaces.

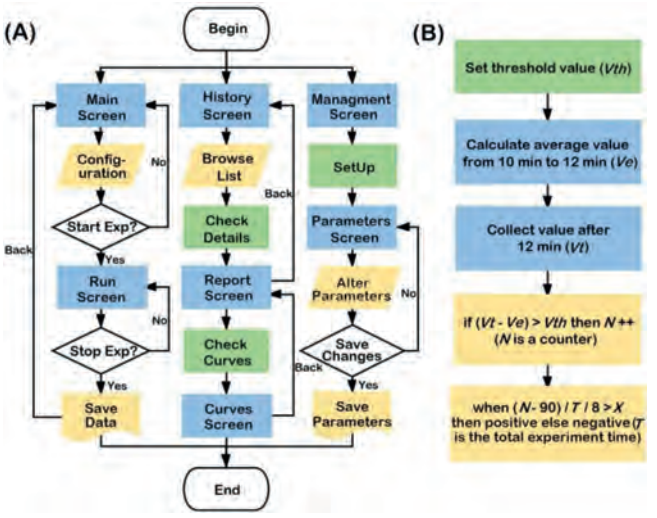

Fig. 2. (A) flowchart of touch screen interface. (B) flowchart for judgment result. *Ve* is the average value during 10–12 min. *Vt* is the current value after 12 min. *Vth* is the threshold for judging whether the curve takes.

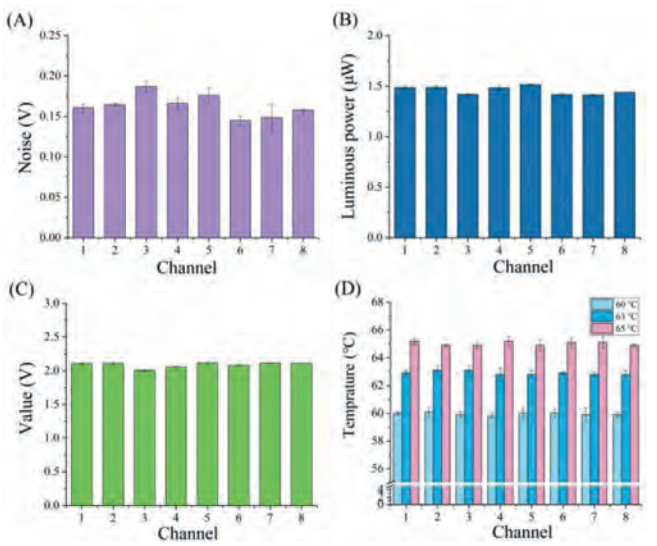

Fig. 3. (A) Background uniformity. (B) Luminous power uniformity. (C) Eight PCR tubes filled with water. (D) Temperature uniformity.

low detection efficiency, making detection and identification difficult. In contrast, molecular techniques serve as feasible alternatives and possess the advantages of high sensitivity, good specificity, and rapid detection. At present, more novel detection methods appeared including chemiluminescence immunoassay, polymerase chain reaction (PCR) [8–10], real-time fluorescence quantitative PCR [11–13], aptamer [14–17], hybridization [18,19], electrochemical biosensor [20–22] and loop mediated isothermal amplification (LAMP) [23–31], and so on. The immunity-based method has very high sensitivity [32,33], but stability of reagent is poor and the structure of equipment and instrument is complex. PCR-based method has the disadvantages of complicated operation and high cost of instruments and reagents, which limits its field application [34]. Sensors-based method has smaller size and high sensitivity, but the lifespan is short. However, LAMP does not require a thermocycler and needs only simple instruments and a relatively short time period to perform the amplification with high sensitivity and specificity [35]. Subsequently, the amplification result can be judged based on agarose gel electrophoresis, metal indicator (Hydroxynaphthol blue), fluorescence probe (SYBR Green I), or turbidity (Magnesium pyrophosphate precipitation) [36,37]. Of these, the turbidity detection is a very simple, fast, accurate, low-cost, and pollution-free method for early on-site EHP diagnosis. Nonetheless, relying on the naked eye for result interpretation easily leads to misjudgments, and the fluorescence device is expensive and complex to operate. Moreover, the main detection preforms are microfluidic chip [38,39], cartridge [40], paper [41], tubes [42,43], and the different preforms have different features. This paper provided a novel thermostatic nucleic acid testing device for monitoring the variation of magnesium pyrophosphate precipitation in tubes, and test for EHP.

In LAMP, the target gene is amplified at a constant temperature of 60–65 °C using Bst DNA polymerase within 1 h. The amplified products can be measured by turbidity generated from magnesium pyrophosphate during strand displacement, which can be used to indicate the process and state of the reaction [44,45]. The light-absorbing of the solution is related to the concentration of the turbidity, and can be determined by Beer's law (Eq. 1) [46]:

$$A = \lg\left(\frac{I_R}{I_T}\right) \quad (1)$$

where, A is absorbance, I_R is the incident light intensity, I_T is the transmitted light intensity.

The design of the diagnostic device is shown in Fig. 1A. The entity graph ($18.8 \times 16.7 \times 6.6$ cm^3) consists of four parts: heating cover module (Fig. 1B), reaction module (Fig. 1C), touch screen interfaces (Fig. 1D and Fig. S6 in Supporting information), and outer covering [47]. The core of the device is the reaction module, which consists of the laser diode (LD), thermal insulation (INS), photodiode (PD), aluminum block (ALB), heater, and heater pad. The LD and PD are separately controlled by a silicon photodiode (Si-PD) detection-based printed circuit board (PCB) and laser driven PCB. The LD sends out constant power light under the control of the drive circuit as the incident light source. The PD can convert the change of transmitted light intensity into the change of the voltage value. Therefore, it can monitor the turbidity of mixture solution in real time by collecting the voltage value. The heater provides constant temperature for the LAMP reaction [42]. To prevent the liquid from evaporating, the heating cover module is equipped with springs, ALB, thermal fuse, heater, INS, and the top lid. For enhanced user experience, simple and practical screens are used, including the home screen, the run screen, the history screen, and the report screen. The inspector needs to merely input the name of the experiment, the number of samples, and the temperature and time of reaction and then press "START". The device can run, judge, and show the results in an automated manner within 1 h.

Seven touch screens were designed for the operator to easily use the device. As shown in Fig. 2A, when the device is pow-

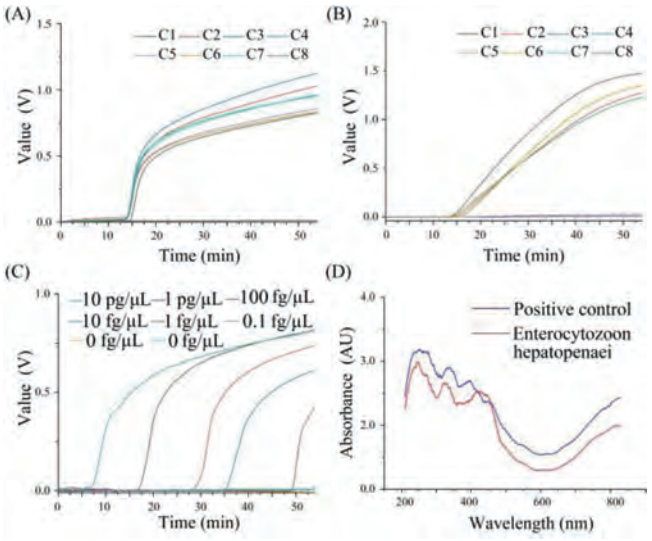

Fig. 4. (A) Seven positive and one negative samples. (B) Four positive and four negative samples. (C) Sensitivity test by different concentrations of samples. (D) Absorbance test by ultraviolet-visible near infrared spectrum.

ered, the first screen called "Main Screen" is shown and the operator can set the parameters (for example, experiment name and experiment condition) in this screen. If the "Start Exp" button is pressed, the experiment commences. The "Run Screen" shows the dynamic experiment curves and experiment temperatures in real time. Once the experiment ends, all data are saved to the secure digital memory card automatically, which can be viewed in the "History Screen." In addition, the calibration parameters can be updated and read in the "Management Screen."

The flow of the judgment algorithm (Fig. 2B) for the experiment is implemented by the touch screen. The program collects the voltage value of one channel by 8 s, calculates the average value (*Ve*) of each channel from 10 min to 12 min as baseline value, then timely collects the value (*Vt*) after 12 min. If the difference between *Vt* and *Ve* is greater than the threshold (*Vth*) which is used to judge whether the curve takes off, the counter (*N*) will plus one. Finally, the following formula (Eq. 2) is used to judge the results of the experiment:

$$x = \frac{N - 90}{T/8} \tag{2}$$

where, *N* is the time of one channel to maintain the jump. *T* is the total experiment running time, so the running time of a single channel is *T* divided by 8. The value of *x* is the proportion of the time after the take-off of one channel to the running time. When *x* was more than the threshold (*X*) which is used to judge the experimental results, the judgment result is positive, else is negative. By the analysis of fifty sensitive and reacted EHP experiences, the values of *Vth* and *X* are set 1 and 0.1.

The performance evaluation of the device chiefly included temperature, luminous power, background uniformity and stability [42], and EHP testing assay. One thermistor (2.252 kΩ type, Accuthermo Technology Corp.) and thermostat (ATEC302, Accuthermo Technology Corp) were employed to monitor the temperature. The optical power meter (PM100D; Thorlabs Inc.) was used to measure the luminous power. Furthermore, the data acquisition system was used to measure the background from the eight PCR tubes (0.2 mL; Axygen Scientific Inc.) filled with 25 μL of purified water. The total volume of LAMP reaction utilized for EHP detection was 25 μL and was covered with 30 μL of oil in each PCR tube.

Figs. 3A-D depict the evaluation of the uniformity of the system from four important aspects (background, luminous power, values of eight PCR tubes filled with pure water, and temperature). The following results were obtained: (I) The measured noises of the eight channels represent the background uniformity, and the CVV was an average of 3.24% (Fig. 3A). (II) The optical power of the eight channels denotes the luminous power uniformity, and the CVV was an average of 0.7% (Fig. 3B). (III) The voltage signals of the eight channels filled with 25 μL of pure water signify the absorbance uniformity, and the CVV was 0.43% in average (Fig. 3C). (IV) The temperatures of the eight channels at 60 °C, 63 °C, and 65 °C indicate the temperature uniformity, and the average CVVs were 0.48%, 0.43%, and 0.38%, respectively (Fig. 3D). The CVVs of every eight channels were less than 5% in the uniform testing experiments (Table S2 in Supporting information). The above results demonstrated that the established system has very good uniformity.

In Fig. S4A (Supporting information), the three curves demonstrate the temperature stability (at 60, 63, and 65 °C) in one channel with one PCR tube containing 25 μL of purified water and 30 μL of oil and inserted with a thermistor-based temperature sensor. The heating speed was about 1 °C per second, and the precision of temperature control was less than 0.2 °C. In Fig. S4B (Supporting information), at 63 °C, these curves showed stability in eight PCR tubes filled with 25 μL of purified water. The maximum and minimum values of CVV were 0.82% and 0.045%, respectively, which were much less than 5%. The above results alluded that this system has very good stability. In Fig. S5 (Supporting information), the curve signifies the stability of the luminous power in one channel when the light was turned on and off. The fluctuation values were 0.0097 and 0.0014, respectively, within 1 h.

We designed three groups of experiments to verify the EHP detection capability of the device. (I) Eight samples (seven are positive and one is negative) were used to verify the effectiveness of the device. (II) Four positive and four negative samples were used to verify the device effectiveness and the existence of cross-contamination. (III) Eight samples (six are positive samples diluted from 10 pg/μL to 10^{-4} pg/μL and two are negative samples) were used to verify the sensitivity of the device. The curves of the results were shown in Fig. 4. Seven curves were takeoff and have similar trends, imply that the device has good uniformity and stability (Fig. 4A); Four positive were takeoff, and others were not, that indicated there was no cross-contamination (Fig. 4B); As the concentration of positive samples decreased, the take-off time of the curve was also delayed, and the lowest detection limitation was 0.1 fg/μL (Fig. 4C). Besides, all positive samples can be correctly judged by the designed algorithm.

For finding the optimal absorbance wavelength, we designed a positive control group and EHP experimental group by LAMP. Absorbance spectroscopic tests were performed at 200–800 nm using ultraviolet-visible-near infrared spectrum (Lambda 750S, PerkinElmer). As illustrated in Fig. 4D, the optimal and minimum absorbance range was 555–655 nm. In this range, the absorbance value of the solution was accurate because there was less interference from impurities. In market, most lasers have standard wavelengths (such as 520, 650, 670 nm) [48]. Hence, we chose a 650 nm laser.

In this work, we have been developed a new on-site rapid testing device for EHP with good stability and high uniformity. We find that the better absorbance detection range of the product of LAMP was 555–655 nm. The adoption of laser diode with monochromaticity and unipolarity improves the stability and accuracy of the signals. Besides, an automatic semi-quantitative judgment algorithm has provided for judging the result is positive or negative and verified the precision through lots of experiments. In summary, this device exhibited very good stability, uniformity, and

reliability. Owing to the ease of operation and the high accuracy for EHP detection, this device can find widespread applications in the rapid detection of nucleic acids in primary community hospitals, customs, *etc*.

Declaration of competing interest

We declare that we have no financial and personal relationships with other people or organizations that can inappropriately influence our work, there is no professional or other personal interest of any nature or kind in any product, service and/or company that could be construed as influencing the position presented in, or the review of, the manuscript entitled.

Acknowledgments

This work was supported by the grant from the National Natural Science Foundation of China (Nos. 61901168, 61971187, 61871180, 82002405), Hunan Key Research and Development Program (No. 2021SK2003), Zhuzhou Innovative City Construction Project (No. 2020–020) and China Postdoctoral Science Foundation (No. 2018M630498).

Supplementary materials

Supplementary material associated with this article can be found, in the online version, at doi:10.1016/j.cclet.2022.01.072.

References

[1] S. Thamizhvanan, S. Sivakumar, K.S. Santhosh, et al., J. Fish. Dis. 42 (2019) 447–454.
[2] T. Chaijarasphong, N. Munkongwongsiri, G.D. Stentiford, et al., J. Invertebr. Pathol. 186 (2020) 107458.
[3] P.V. Salachan, P. Jaroenlak, S. Thitamadee, O. Itsathitphaisarn, K. Sritunyalucksana, BMC. Vet. Res. 13 (2017) 9.
[4] K. Karthikeyan, R. Sudhakaran, J. Fish. Dis. 42 (2019) 397–404.
[5] S.X. Cai, F.D. Kong, S.F. Xu, C.L. Yao, PeerJ 6 (2018) e5993.
[6] P. Jaroenlak, P. Sanguanrut, B.A.P. Williams, PLoS One 11 (2016) e0166320.
[7] R. Cruz-Flores, H.N. Mai, B.L. Noble, P.J. Schofield, A.K. Dhar, J. Microbiol. Methods 162 (2019) 38–41.
[8] J.E. Han, S.C. Lee, S.C. Park, et al., Aquaculture 517 (2020) 734812.
[9] J.E. Han, K.F. Tang, C.R. Pantoja, et al., Dis. Aquat. Organ. 120 (2016) 165–171.
[10] P. Piamsomboon, S.K. Choi, B. Hanggono, et al., Pathogens 8 (2019) 233.
[11] B.K. Chen, Z. Dong, N.Y. Pang, et al., J. Invertebr. Pathol. 157 (2018) 100–103.
[12] Y.M. Liu, L. Qiu, A.Z. Sheng, et al., J. Invertebr. Pathol. 151 (2018) 191–196.
[13] L. Wang, Q. Lv, Y. He, et al., Microorganisms 8 (2020) 1366.
[14] Z.K. Guo, Y. Liu, N.Y. He, et al., Chin. Chem. Lett. 32 (2021) 40–47.
[15] X.H. Zhou, Q. Zhu, Y.H. Yang, Biosens. Bioelectron. 165 (2020) 112422.
[16] M. Liu, L. Xi, T. Tan, et al., Chin. Chem. Lett. 32 (2021) 1726–1730.
[17] K.S. Park, Biosens. Bioelectron. 102 (2018) 179–188.
[18] H.M. Dong, C.L. Tang, Z.Y. He, et al., Chin. Chem. Lett. 31 (2020) 1812–1816.
[19] K.F. Tang, C.R. Pantoja, R.M. Redman, et al., J. Invertebr. Pathol. 130 (2015) 37–41.
[20] L. He, R.R. Huang, P.F. Xiao, et al., Chin. Chem. Lett. 32 (2021) 1593–1602.
[21] R. Bruch, J. Baaske, C. Chatelle, et al., Adv. Mater. 31 (2019) 1905311.
[22] Y. Liu, G.J. Yang, T.T. Li, et al., Chin. Chem. Lett. 32 (2021) 1957–1962.
[23] C. Avendano, M.A. Patarroyo, Int. J. Mol. Sci. 21 (2020) 7981.
[24] S. Higashide, O. Cho, Y. Matsuda, et al., Microbiol. Immunol. 62 (2018) 607–611.
[25] T. Huang, L. Li, X. Liu, et al., Anal. Methods 12 (2020) 5551–5561.
[26] D. Selvarajah, C. Naing, N.H. Htet, J.W. Mak, Malar. J. 19 (2020) 211.
[27] S. Waliullah, K.S. Ling, E.J. Cieniewicz, et al., Int. J. Mol. Sci. 21 (2020) 1756.
[28] D. Wang, J. Yu, Y. Wang, et al., J. Virol. Methods 276 (2020) 113775.
[29] J. Xiong, B. Huang, J.S. Xu, W.S Huang, Appl. Biochem. Biotechnol. 191 (2020) 201–211.
[30] J. Yu, J. Xie, Y. Cao, et al., Anim. Biotechnol. 32 (2020) 1–8.
[31] L. Zhang, C. Gleason, Plant. Dis. 103 (2019) 12–18.
[32] H. Zhao, E. Su, L. Huang, et al., Chin. Chem. Lett. 33 (2022) 743–746.
[33] H. Zhao, Q.F. Lin, L. Huang, et al., Nanoscale 13 (2021) 3275–3284.
[34] K.S. Sreedeep, S. Sethi, R. Yadav, et al., J. Infect. Chemother. 26 (2020) 823–830.
[35] T. Kamber, L.L. Koekemoer, A. Mathis, Med. Vet. Entomol. 34 (2020) 295–301.
[36] M. Hussain, X.L. Liu, J. Zou, et al., Chin. Chem. Lett. 33 (2022) 1885–1888.
[37] S.Y. Wang, N. Liu, L.Y. Zheng, G.Z. Cai, J.H. Lin, Lab. Chip 20 (2020) 2296–2305.
[38] L. Huang, E.B. Su, Y. Liu, et al., Chin. Chem. Lett. 32 (2021) 1555–1558.
[39] X.S. Xu, N.Y. He, Chin. Chem. Lett. 32 (2021) 1747–1750.
[40] Y.L. Fang, H.R. Liu, Y. Wang, et al., J. Biomed. Nanotechnol. 17 (2021) 407–415.
[41] Y.Y. Xu, T. Wang, Z. Chen, et al., Chin. Chem. Lett. 32 (2021) 3675–3686.
[42] Z. Chen, T. Yang, H.W. Yang, et al., J. Biomed. Nanotechnol. 14 (2018) 198–205.
[43] M. Hussain, Z. Chen, M. Lv, et al., Chin. Chem. Lett. 31 (2020) 3163–3167.
[44] A. Sappat, W. Jaroenram, T. Puthawibool, et al., J. Virol. Methods 175 (2011) 141–148.
[45] Y.Q. Zhang, X.X. Shan, L. Shi, et al., Food. Res. Int. 45 (2012) 1011–1015.
[46] H. Abitan, H. Bohr, P. Buchhave, Appl. Optics 47 (2008) 5354–5357.
[47] Y. Mori, M. Kitao, N. Tomita, T. Notomi, J. Biochem. Bioph. Meth. 59 (2004) 145–157.
[48] J.K. Jabczynski, R.S. Romaniuk, Laser Technology 10974 (2018) 1097402.